Journal of Scientific & Industrial Research
Vol. 83, August 2024, pp. 845-855
DOI: 10.56042/jsir.v83i8.10192

Exploring Petcoke Fly Ash Characteristics for Wider Application as Cement-Based Composites

Varsha Parmar[1,2]*, Prabha Padmakaran[1,2] & Mohd. Akram Khan[1,2]
[1]CSIR-Advanced Materials and Processes Research Institute, Hoshangabad Road, Bhopal 462 026 (M.P), India
[2]Academy of Scientific and Innovative Research (AcSIR), Ghaziabad 201 002, India

Received 04 April 2024; revised 24 May 2024; accepted 10 July 2024

As country's demand for petroleum coke in power plants is increasing drastically as a substitute for coal due to its high carbon content and easy availability, it results in large generation of petcoke combustion byproducts. Reducing the potential leachability of possible heavy metals from these byproducts is a crucial issue for its safe disposal and proper utilization. In this study, Petcoke Fly Ash (PCFA) and Bed Ash (BA) were characterized for mineralogical, morphological, metal analysis using analytical technique like XRD, SEM, HR-TEM, WD-XRF, FTIR, AAS and leachability studies using TCLP. Results showed mean particle size of PCFA is 18.015 µm and BA is 41.165 µm, leachable concentration of Vanadium, Nickel, Chromium, Manganese, Aluminium, Barium and other heavy metals in both ashes, XRD shows presence of $CaSO_4$, V_2O_5 and CaO, SEM and HR-TEM micrographs confirm that PCFA and BA have porous morphology with varying size and irregular particles with interplanar spacing of 0.35 nm and 0.32 nm respectively. Results also confirmed the resemblance of PCFA with PPC in terms of fineness (PCFA=2960 m^2/g and PPC≥3000 m^2/g, consistency (PCFA 36–45% and PPC 25–35%). The study concluded that based on textural, compositional and mechanical properties, PCFA and BA have potential as an alternative raw material in cement concrete for application in development of low cost, green construction materials.

Keywords: Bed ash, Hydration product, Leachability, Petroleum coke fly ash, TCLP

Introduction

Petroleum coke (Petcoke), a by-product of the petroleum refining process is favored for power generation due to its superior calorific value making it a more efficient alternative to coal.[1] In India, rising the use of Circulating Fluidized Bed Combustion (CFBC) technology is the greatest alternative for higher fuel efficiency and for renovating ageing Pulverized Coal Combustion boilers to extend their life to approximately 20 years and reducing coal imports by effectively using fuels with lower calorific value like lignite.[2] Combustion of petcoke with higher sulphur content as fuel at 900°C in CFBC boilers using limestone as desulfurizing agents results in generation of petcoke fly ash and bed ash. However, co-firing of petcoke and limestone enhances the capture of few heavy metals like nickel, vanadium, chromium, manganese, aluminium, barium and others into the ash, thereby mitigating the risk of secondary pollution from these heavy metals.[3,4] Bed material is also used in the boiler to support fluidization of the bed which is high gravity sand that allows uniform air distribution for proper fluidization and ensuring excellent turbulence for combustion with minimum access to air. The desulfurized petcoke by-product is classified into two types: desulfurized petcoke fly ash, which is collected from silos and bed ash which is the waste residue remaining at the bottom of the boiler bed.[5]

Approximately 5.0 million tons of petcoke fly ash is generated annually in industrial sectors of M.P, India which poses great environmental challenge in terms of proper utilization and disposal.[6] Significant amounts of PCFA are typically disposed off in ash dump yards resulting in considerable land usage and environmental pollution. The vast accumulation of this waste materials adversely affects both the environment and human health hence there is an urgent need for its proper utilization and disposal in scientific manner. To ensure reliability and nature of the raw materials, knowledge of extensive characterization in terms of mineralogical, morphological, elemental, heavy metal composition and its hazards in terms of leachability of material is very crucial.

Presently, the use of CFBC technique has increased due to co-firing of blended fuel which results in high

---

*Author for Correspondence
E-mail: varshaparmar.vp15@gmail.com

variation in the generated fly ash quality. Previously, Ohenoja *et al*., 2020(7) reported the different applications of fly ash from fluidized bed combustion. Jia *et al*., 2022(8) reported the application of fly ash from coal combustion from CFBC boiler. Some more research papers have extensively discussed the physico-chemical properties of CFBC ash, as well as its current and potential future applications.[9,10] Nevertheless, there is a significant gap in the literature concerning the comprehensive characterization and application of CFBC fly ash produced exclusively from 100% petcoke combustion. The aim of this study is to carry out comprehensive characterization of PCFA and BA by applying different characterization techniques in order to gain basic information for finding the future potential application of these waste materials through useful products in the field of construction and civil engineering applications.

Materials & Methods

Sample Preparation

Samples of PCFA and BA generated from CFBC boiler as shown in Fig. 1 were collected from the Captive Power Plant (CPP) of major Oil Refinery located in Madhya Pradesh, Indiain CFBC boiler fed with 100% petcoke. After collection, the samples were dried at 105°C for 24 h in microprocessor controlled hot air oven followed by cooling to achieve a constant weight by removing moisture. Samples were gently ground using mortar & pestle and powdered sample is used for further characterization. Study was carried out in two parts; first part comprised of physico-chemical characterization of PCFA and BA and second part comprised of comparison of PCFA with PPC in terms of cementitious properties through mortar samples as per Indian Standard (IS). However, sufficient literature is not reported for utilization of bed ash in cement replacement.

In CFBC boiler, PCFA and BA generation involves several key processes as shown in Fig. 2. Initially, during devolatilization, the fuel undergoes pyrolysis in the dense bed of the boiler, releasing volatile compounds like hydrocarbons, tar and methane at temperatures of 400–600°C. These volatile compounds are then heated to higher temperatures (800–900°C) in the freeboard zone, where they are converted into gases such as carbon monoxide, carbon dioxide and hydrogen. As the flue gas carries fine ash particles and unburnt carbon, they collide with each other and the walls of the boiler, leading to collision and agglomeration, forming larger clusters of particles. Additionally, the circulating bed of sand and limestone causes abrasion and attrition of fuel and ash particles, generating finer particles those are carried away with the flue gas. Moreover, some ash particles are formed within the bed through chemical reactions between fuel components and the bed material, further contributing to ash generation.[11]

Physico-chemical Properties

Physico-chemical characterization like pH was determined using pH meter make pHep, HANNA using aqueous solution in 1:10 ratio. Blain Fineness was determined using Blaine Air Permeability Test (AIM 390) make AIMIL as per IS 4031–1999.(12) Bulk density and Particle density were determined as per IS 2720– 1980, Reaffirmed 2002(13) using RD bottle. Moisture content was determined using oven drying method in accordance with IS 2720–1973, Reaffirmed 1997.(14) Particle size distribution curve for PCFA ad BA were analyzed through Laser

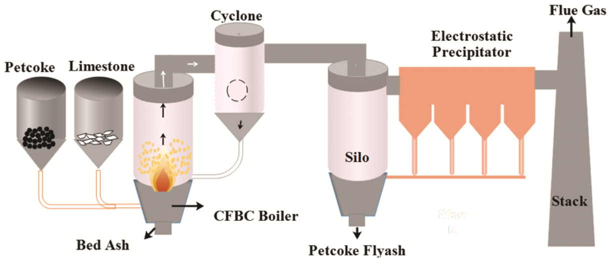

Fig. 1 — Schematic diagram of CFBC boiler

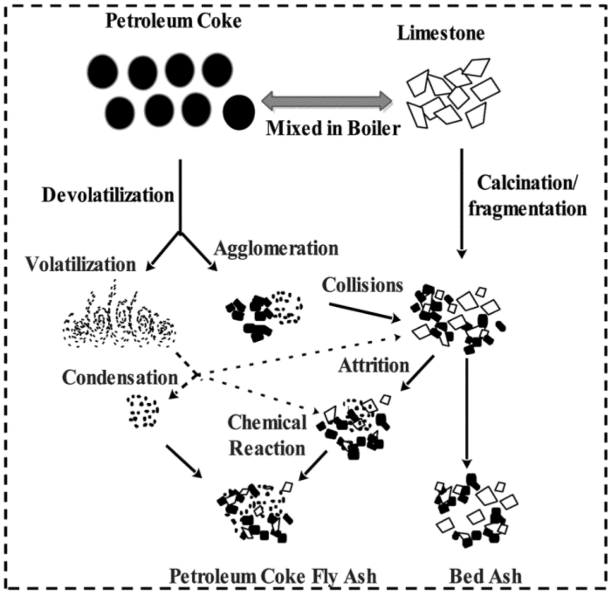

Fig. 2 — Mechanism of ash generation in CFBC boiler

Scattering Particle Size Distribution Analyzer (Make HORIBA Scientific Model Partica LA– 950). Loss on Ignition (LoI) was performed as per IS: 1727–1967, Reaffirmed 2004(15) @ 900°C for 1 Hour.

Chemical Composition by X-Ray Fluorescence (XRF)

Sample pellets of 40 mm diameter were prepared along with boric acid to determine elemental composition using Wavelength- Dispersive X-Ray Fluorescence (WDX-XRF), Make S8 TIGER BRUKER, Germany. The results were obtained for major elements like Calcium, Sulphur, Aluminium, Iron, Silicon, Titanium, Barium, Sulphur, Magnesium, Vanadium, Sodium and Potassium in the form of oxides.

Mineralogical Studies

The X-ray Diffraction (XRD) patterns of PCFA and BA were obtained using a Rigaku MiniFlex II Desktop with CuKα (λ = 1.5419 Å) radiation. The diffraction patterns were collected over a 2θ range of 10º to 80º with a step size of 0.02° and a total scan time of approximately 30 minutes.

Morphological Studies

Morphological studies were conducted using Scanning Electron Microscope (SEM) Model JEOL JCM 6000 plus and High-Resolution Transmission Electron Microscopy (HR-TEM) Model Jeol TEM F-200. For SEM analysis, the samples were sonicated and sprayed onto carbon tape followed by coating. The sample made conductive by applying deep gold coating in high vacuum mode. Morphological images were captured at a resolutions and magnification of 10 µm and 2000× respectively. In HR-TEM, the samples were prepared by suspending the particles in ethanol and subjecting them to agitation in an ultrasonic bath for 15 minutes. Subsequently, 5 µl of the ash particle sample was deposited onto a copper mesh grid. The wet sample then dried under IR radiation for 3–4 hours before being examined under HR-TEM.

Infrared Spectroscopy Analysis

The Attenuated Total Reflectance-Fourier Transform Infrared Spectroscopy (ATR-FTIR) of PCFA and BA was conducted using FTIR instrument (Make Thermo Scientific Model iS50). The samples were prepared as KBr pellets. Transmittance IR spectra were recorded over the range of 400–4000 cm^{-1} with a resolution of 4 cm^{-1} using 64 scans for each sample.

Total Metal Analysis & Leachability Studies

Total Metal Analysis of PCFA and BA was analyzed using Atomic Absorption Spectrophotometer (AAS), Thermo Fisher Scientific iCE 3000 series. Samples were digested on hot plate using HNO_3 as per USEPA method 3050B, 1996.(16) The leachability of heavy and toxic elements from PCFA and BA were determined using Toxicity Characteristics Leaching Procedure (TCLP) according to EPA 1311 Method, 1992.(17) The equipment setup for TCLP is shown in Fig. 3. The collected leachate from TCLP was analyzed in AAS for heavy metals detection.

Lime Reactivity

Lime reactivity of PCFA was determined as per IS 1727-1967.(15) The mortar specimens of 50 mm were prepared using PCFA, lime and sand in proportion of 1:1.61:9 calculated using $1{:}\,2M{:}\,9$ where, $M =$ (Specific gravity of Pozzolana/ Specific gravity of lime).

Consistency and Compressive Strength

Standard consistency of PCFA was measured as per IS 4031-1988, Reaffirmed 2005(18) using Vicat apparatus to determine the water required in volume (based on PCFA quantity) to make standard consistency of cement.

The mortar samples of size (7 × 7 × 7) cm^3 were prepared using PCFA as per mortar mix 1:3 wherein one part consists of PCFA and three parts consist of sand and were tested using Compression Testing Machine (AIM 320E-DG-1-T) make AIMIL conforming loading rate of 1000 N/s by taking average of three mortar specimen of size (7 × 7 × 7) cm^3 as per IS 4031-1988, Reaffirmed 2000.(19) After casting, specimens were placed under ambient curing conditions for 24 hrs. After demoulding, mortars testing were done for 3, 7 and 28 days.

Results and Discussion

Three observations were recorded for the sample of PCFA and BA for all the parameters and the mean value is reported as below:

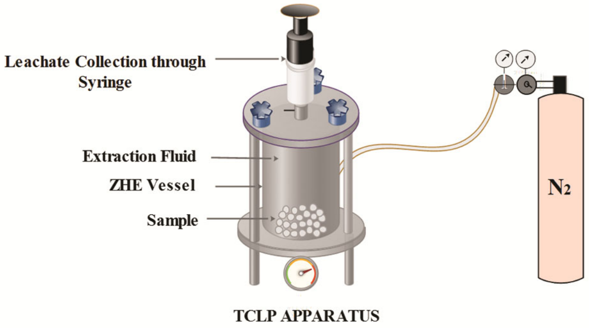

Fig. 3 — Experimental setup of TCLP apparatus

Physico-chemical Properties

The physical parameters of PCFA and BA were determined by adopting standard procedure and are given in Table 1. The color of PCFA is greyish white while silt textured BA is brown in color. The whitish color of PCFA is due to desulphurization process whereas brown color of BA is due to bed material. The pH of PCFA and BA was found to be 12.7 and 12.4 respectively which shows that these are highly alkaline in nature because of presence of higher calcium content**.** The moisture content of PCFA and BA was calculated through Eq. 1, which was found to be 1.24% and 0.03% in PCFA and BA respectively. Owing to the fine particle size of PCFA, it has ability to absorb moisture. The bulk density for PCFA and BA was calculated using Eq. 2 and were found to be 1.27 g/cc and 1.61 g/cc for PCFA and BA respectively. The particle density was calculated using Eq. 3 and it was found to be 2.62 for PCFA and 2.65 for BA. Mean particle size of PCFA and BA was determined as 18.01 µm and 41.16 µm respectively.

$$Moisture\ Content\ (\%) = \frac{W_1 - W_2}{W_2} \qquad \text{... (1)}$$

where, w_1 and w_2 are the weight of original sample (before drying) and weight of sample after oven drying

$$Density\ (g/cm^3) = \frac{Mass}{Volume} \qquad \text{... (2)}$$

$$Particle\ Density\ (\rho) = \frac{W \times \rho^k}{W + W_4 - W_3} \qquad \text{... (3)}$$

where, W is weight of material to be tested ($W = W_2 - W_1$), W_1 is weight of dry RD bottle with stopper, W_2 is weight of RD bottle with sample, W_3 is weight of RD water with sample and measuring liquid, W_4 is weight of closed RD bottle with measuring liquid and ρ^k is the density of measuring liquid at tested temperature.

Particle Size Distribution

The particle size distribution curve of PCFA and BA are depicted in Fig. 4. The result shows that the mean particle size of PCFA was found to be in the range of 16.79–19.23 µm whereas that of BA was found to be in the range of 32.64–49.68 µm. The blue curve indicates the undersize volume (%) and pink curve indicates cumulative percentage (q%) with respect to particle size of PCFA and BA. The results of PCFA (d_{10} 7.64 µm, d_{50} 13.56 µm, d_{90} 28.08 µm) indicate that 10% of the total volume has diameter ≤ 7.64 µm, 50% of the total volume has diameter ≤13.56 µm and 90% of the total volume has diameter ≤ 28.08 µm respectively whereas for BA d_{10} 10.77 µm, d_{50} 29.90 µm, d_{90} 57.013 µm) indicates that 10% of the total volume has diameter ≤ 10.77 µm, 50% of the total volume has diameter ≤ 29.90 µm and 90% of the total volume has diameter ≤ 57.013 µm respectively. However, increased fineness leads to enhanced hydration of lime and anhydrite along with increased dissolution of alumina and silica. This process results in the formation of calcium silicate hydrate gel, ettringite and gypsum. Consequently, a higher content of SO_3 and CaO in finer particles contributes to improved hydration efficiency.[3]

Table 1 — Physico-chemical characterization of PCFA and BA

Parameters	Petroleum coke fly ash	Bed ash
Color	Greyish white	Brown
Texture	Fine grained	Coarse grained
pH	12.7	12.4
Mean Particle size (µm)	18.01	41.16
Bulk density (g/cc)	1.27	1.61
Particle density	2.62	2.65
Moisture content (%)	1.24	0.03

Chemical Composition

The chemical composition of PCFA and BA determined through XRF is dominated by CaO and SO_3, constituting 37.5% – 46.1% and 28.2% – 48.7%

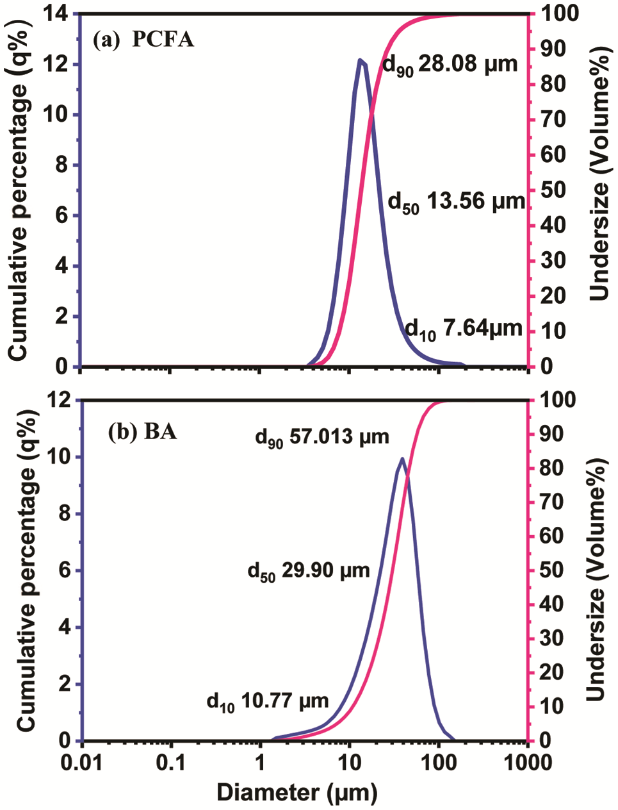

Fig. 4 — Particle size distribution (a) PCFA (b) BA

respectively along with SiO_2, V_2O_5, TiO_2, Al_2O_3 as shown in Fig. 5. The higher content of SO_3 and CaO is due to desulphurization process through addition of limestone in CFBC boiler. Loss on Ignition (LoI) is calculated using Eq. 4 and found to be 8.99% and 10.12% for PCFA and BA respectively. The physical characteristics of petcoke component in bed ash serve as confirmation of higher LoI in BA.

The CFBC boilers operate under sub-stoichiometric conditions to control the combustion temperature and NOx emission. This can lead to incomplete combustion of carbonaceous material resulting in higher levels of unburnt carbon, which is mainly responsible for higher LoI. However, the higher content of SO_3 and CaO are favourable for intensifying the self-cementitious property.[20] Further, it has been shown that the hydration products of the aforementioned active component lead to the formation of portlandite, gypsum, calcium silicate (C-S-H) and ettringite.[21,22]

$$Loss\ on\ Ignition\ (LoI) = \frac{A}{B} \times 100 \qquad \ldots (4)$$

where, A = loss in weight, and B = weight of moisture free sample

Mineralogical Studies

The mineralogical phases obtained in XRD pattern of PCFA and BA as given in Fig. 6 are crystalline phases indexed with JCPDS file for inorganic minerals. The result shows the presence of mineral phases like Anhydrite ($CaSO_4$) (JCPDS No. 6-226), Lime (CaO) (JCPDS No. 4-777), Quartz (SiO_2) (JCPDS No. 33-1161), Calcite Syn ($CaCO_3$) (JCPDS No. 24-27), Iron Vanadium Oxide ($FeVO_4$) (JCPDS No. 31-1438) and Vanadium Oxide (V_2O_5) (JCPDS No. 19-1398) in PCFA whereas Anhydrite ($CaSO_4$) (JCPDS No. 6-226) and Vanadium Oxide (V_2O_5) (JCPDS No. 19-1398) in BA. Anhydrite is created during the desulfurization process, which involves sulphur dioxide adsorption on lime. It was noted that PCFA also contains trace amount of calcite ($CaCO_3$) and free CaO which may be due to the addition of limestone as a desulfurizing agent along with the fuel (petcoke) during the combustion in CFBC boiler.

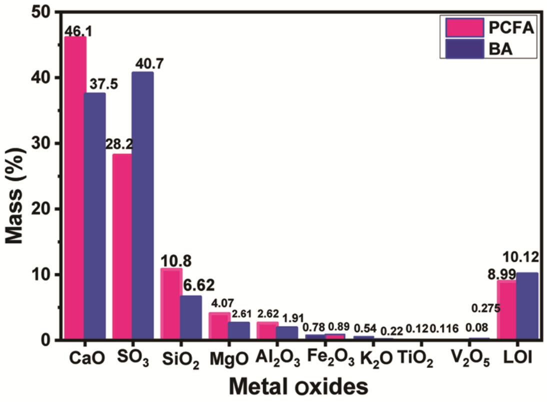

Fig. 5— Chemical composition of PCFA and BA using XRF

The XRD spectrum displayed in Fig. 6 was utilized for crystal phase identification. A significant peak detected at 2θ = 25.21 and 2θ = 25.36 in PCFA and BA respectively which correlates with (020) plane of Calcium Sulphate Anhydrite. The interplanar spacing (d value) was determined to be 0.35nm in both the samples using Bragg's formula $n\lambda = 2dSin\theta$ where, n=1, λ(CuKα) = 1.54Å and θ= 12.605 and θ = 12.68 for PCFA and BA respectively at the highest peak.

The PCFA and BA shows certain amount of self-hardening property due to the presence of lime, anhydrite, cementitious minerals and amorphous matter that allows it to be utilised as a cementitious material. Based on the literature, it can be noted that the hydration phases involved with these components are based on the following reactions:[22–24]

1. Hydration of lime ($CaO + H_2O \rightarrow Ca(OH)_2$)
2. Formation of gypsum ($CaSO_4 + 2H_2O \rightarrow CaSO_4.2H_2O$)
3. Formation of Ettringite due to the reaction of calcium hydroxide and gypsum with alumina

$$(Ca(OH)_2 + 3CaSO_4.2H_2O + 2Al_2O_3 + 8H_2O \rightarrow Ca_6(Al_2SO_4)_3(OH)_{12}.26H_2O)$$

4. The reaction of active silica and calcium hydroxide results in the formation of calcium silicate hydrate gel in the presence of moisture ($SiO_2 + Ca(OH)_2 + H_2O \rightarrow C - S - H$)

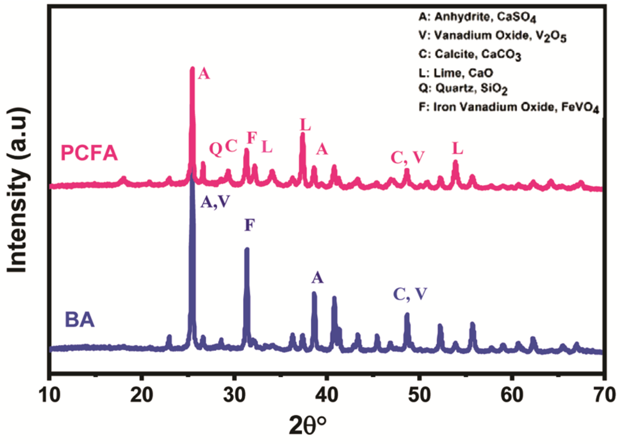

Fig. 6 — X-ray diffraction pattern of PCFA and BA

Fourier Transform- Infrared Spectra

The ATR-FTIR spectra of PCFA and BA are as shown in Fig. 7. Narrow peaks in molecular bands indicate a highly crystalline structure, while broader peaks indicate an amorphous structure. The broad intense sharp bands are near 1097 in PCFA and 1119 cm^{-1} in BA. Moderate intense but distinctive bands at 594, 611, 676 cm^{-1} in PCFA and at 594, 612, 678 cm^{-1} in BA corresponds to the bending and stretching of S-O in SO_4^{2-} ion which indicates the presence of Anhydrous Calcium Sulphate. The characteristic band at 2933 cm^{-1} corresponds to the vibration mode of C-H which indicate the extent of carbon content in the in PCFA and BA. The vibrational modes of CO_3^{2-} associated with carbonates, specifically the out-of-plane bending at 870 cm^{-1} and the asymmetric stretching at 1457 cm^{-1} were also detected and identified in BA.[25] In PCFA, a moderately intense band at 1411 cm^{-1} signifies C-O stretching, while the band at 873 cm^{-1} indicates C-O out-of-plane bending, indicating the presence of carbonates as calcite ($CaCO_3$), whereas the band at 797 cm^{-1} corresponds to the Si-O vibration of Quartz.[26] In BA a distinct band at 3642 cm^{-1} has attributed to the O-H vibration in portlandite. The presence of sharp and intense band confirmed the crystalline nature of PCFA and BA while the resemblance between the identified functional groups and the crystal phases revealed in XRD analysis further validates the structural composition of both PCFA and BA.

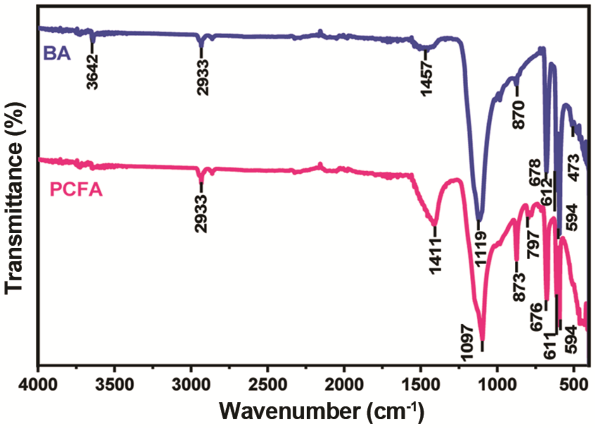

Fig. 7 — FTIR analysis of PCFA and BA

Morphological Studies

Scanning Electron Microscope (SEM)

The morphological study of PCFA and BA as shown in Fig. 8 was carried out ata scale of 10 µm and magnification of 2000x. PCFA particles exhibit irregular shapes, resembling vesicles or having a sub-angular to angular structure typical of anhydrite, with rough surfaces and varying sizes. The particles may agglomerate due to the condensation and deposition of volatile species on their surfaces. Some petcoke constituents may not melt completely, leading to the formation of non-spherical particles due to rapid cooling of viscous melt droplets and surface energy.[3,27] The cementitious characteristics of PCFA can be observed on FTIR spectra in the form of the presence of carbonate (C-O) and (Si-O) functional group. This morphology of PCFA is similar to the one observed by Pei *et al*., 2023(27), Kleinhans *et al*., 2018.(28) The microstructure of Bed Ash (BA) clearly shows loose and porous structure. In CFBC boiler temperature gradient does not allow melting of irregular shaped ash particles to spherical resulting in loose surface porous structure. Due to porous morphology and high lime content, it has higher water requirement for normal consistency as compared to portland pozzolana cement.[24] This characteristic is also evident in the FTIR spectra, where the presence of hydroxyl (OH) functional groups is observed. Hence, PCFA shows more favourable microstructure

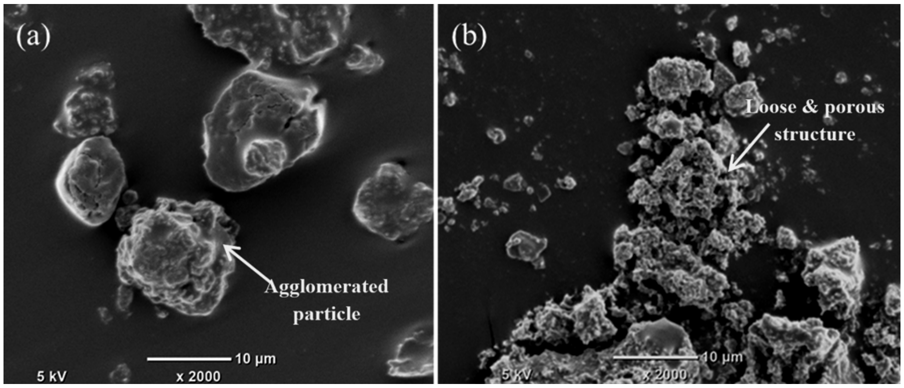

Fig. 8 — SEM images of (a) PCFA (b) BA

for use in construction applications as pozzolanic material than BA.

High Resolution-Transmission Electron Microscope (HR-TEM)

A high-resolution transmission electron microscope (HR-TEM) was employed to examine the structure and crystallinity of PCFA and BA particles. The high-resolution images, size and shape of PCFA and BA were observed using an HR-TEM (Make: JEOL, Model: JEM-F200). The samples were prepared over a carbon-coated copper grid (400 mesh) (Ted-Pella Inc., Redding, CA, USA). The morphological analysis was conducted using HR-TEM as shown in Fig. 9.

The particles of PCFA have an extremely erratic shape which appear to be agglomerated in amorphous matrix. These particles are opaque with darker areas indicating thicker material layers and lighter areas indicating thinner layers within the image. Similar results for TEM analysis were reported by Singh *et al.*, 2023(29) and Tomasz *et al.*, 2021.(30) The BA particles showed irregular structured flocs with varying size. The particles of BA are seen to be loose and scattered. Mineral particles have various irregular shapes which may consist of spherical particles of SiO_2, $CaSO_4$ or some unburnt petcoke particles which are confirmed through XRD spectra.

The lattice fringes (Fig. 9c & d) were calculated at 10 nm scale and the interplanar spacing of petcoke fly ash was found to be 0.35 nm (3.5Å), confirming the (020) hkl plane while d-spacing in the bed ash was found to be 0.32 nm (3.2 Å) that can be attributed to (020) hkl plane. The TEM findings were in agreement with the calculated XRD data. The perfectly parallel lattice fringes confirm that the particle of PCFA and BA are free from lattice imperfections.

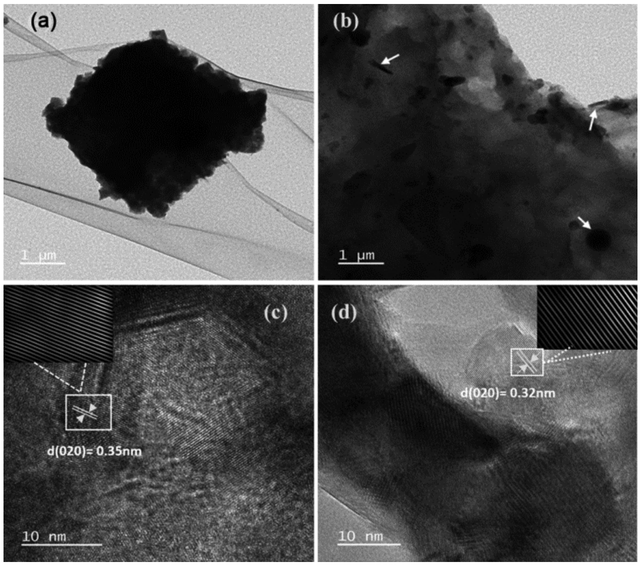

Fig. 9 — (a) HR-TEM image of PCFA (b) HR-TEM image of BA (c,d) Magnified fringes pattern of PCFA & BA

Total Metal Analysis & Leachability Studies

The heavy metals in PCFA and BA were analyzed and reported in mg/L for elements like Iron, Lead, Zinc, Copper, Aluminium, Chromium, Cadmium, Cobalt, Manganese, Vanadium, Barium and Nickel as given in Table 2. The results showed presence of Iron, Lead, Zinc, Copper, Aluminium, Chromium, Manganese, Vanadium and Barium with higher concentrations of Lead, Aluminium, Vanadium, Manganese and Barium. Results showed that the concentration of heavy metals were comparatively higher in PCFA than BA as the major constituents of petcoke reflect in PCFA. The heavy metals present in ashes are mainly contributed from the petroleum coke and other materials like limestone and bed material.

The leachability studies of PCFA and BA were done using TCLP in 25 gm of sample as per standard procedure. The sample was poured in zero head space extractor with capacity of 500 mL containing extraction fluid of NaOH and glacial acetic acid inacidic media (pH 4.93 ± 0.05). The primary leachate was collected from ZHE vessel using syringe of 50 mL at a requisite pressure of 50 psi through N_2 gas. The collected leachates were analyzed for elements as indicated in Fig. 10. The leachate concentration detected through AAS in different ashes showed the presence of Iron, Lead, Zinc, Copper, Aluminium, Manganese, Vanadium, Barium and Nickel elements. However, the detected heavy metals are well within the permissible limits which confirm that PCFA and BA are non-toxic and environmentally safe to be used as pozzolanic material for construction application.

Table 2 — Total metal analysis of PCFA and BA

Elements	PCFA	BA
Fe	2584.0	2013.0
Pb	14.28	7.87
Zn	21.18	33.01
Cu	5.56	2.54
Al	5500.0	1473.0
Cr	21.67	26.83
Cd	BDL	BDL
Co	BDL	BDL
Mn	105.28	73.64
V	1042.6	2574.8
Ba	345.7	195.7
Ni	131.0	240.0

All values are in mgL^{-1}, BDL signifies Below Detection Limit

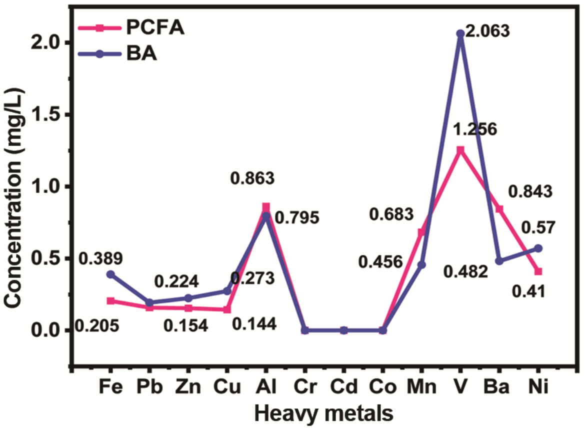

Fig. 10 — Leachability studies of PCFA & BA

Table 3 — Comparative properties of PCFA and PPC

Properties	PCFA	PPC
Specific gravity	2.62	2.90
Blaine fineness (cm^2/g)	3040	Not less than 3000
Particle Size (µm)	16.79–19.23	10–20
Consistency (%)	46.6	25–35
Lime reactivity (MPa)	8.6	Not less than 4
Compressive strength (MPa)		
3 day	14.90	16.0
7 day	21.50	22.0
28 day	38.90	33.0
Hydration product	Calcium silicate Hydrate gel, Portlandite, Gypsum, Ettringite	Calcium Silicate Hydrate Gel, Portlandite, Ettringite

Pozzolanic Properties of PCFA

The pozzolana properties like specific gravity, Blaine fineness, lime reactivity, consistency, compressive strength and hydration products of PCFA mixture are evaluated using standard procedures/techniques and compared with the properties of Portland Pozzolana Cement as per IS 1489–1991, Reaffirmed 2002(31) as shown in Table 3. The specific gravity of PCFA was found to be 2.62 which was found comparable with PPC with 2.90 and the fineness measured by Blaine air permeability apparatus applying Eq.5, was found to be 3040 cm^2/g which is compatible with the pozzolana characteristics of PPC. The pozzolanic properties of PPC are influenced by its fineness. The finer the pozzolana material, the more significant is its surface area for hydration, leading to accelerated strength development. The PCFA particle size distribution was found to bed$_{10}$ = 7.64 µm, d_{50} = 13.56 µm, d_{90} = 28.08 µm whereas the average particle size of PPC lies between 10–20 µm (d_{50} 18 µm) The PCFA was significantly coarser than the cement, although it is meeting fineness criteria for pozzolana materials as per IS.

Fig. 11 — Mortar sample from PCFA and PPC

$$Blaine = k\sqrt{t} \quad \dots (5)$$

where, k is 523.0547 and t is the time recorded of dropping oil level (2.41s)

The water requirement for consistency of PCFA was found to be 46.6% which is approximately 12% higher than the limit of pozzolanic material. The increased water need is in agreement with the sub-angular form and interior porosity of PCFA morphology.[10] The paste consistency of cementitious mixtures containing PCFA was measured through cylindrical specimen of diameter 150 mm and height 150 mm using the Vicat Apparatus to get the information about mixture behaviour over the time and its suitability for different construction applications. The initial and final setting time of PCFA based paste were determined using Vicat Apparatus as per ASTM C191.(32) To determine the initial setting time of PCFA, 500 gm of PCFA paste were prepared with a standard water-to-PCFA ratio followed by filling the Vicat mold with the paste and level the surface, the recorded time was 220 min at depth of 5 mm ± 1 mm whereas the recorded final setting time was 360 min at depth of 30 mm ± 1 mm.

The mortar cubes of size (7 × 7 × 7) cm^3 were prepared from PCFA and PPC as shown in Fig. 11. After demoulding, the specimen were kept for water curing and subsequently tested for compressive strength. The compressive strength versus age of the mortar sample is as shown in Fig. 12. At 3, 7 and 28 days, the compressive strength of the PCFA based mortar sample were comparable to PPC samples and

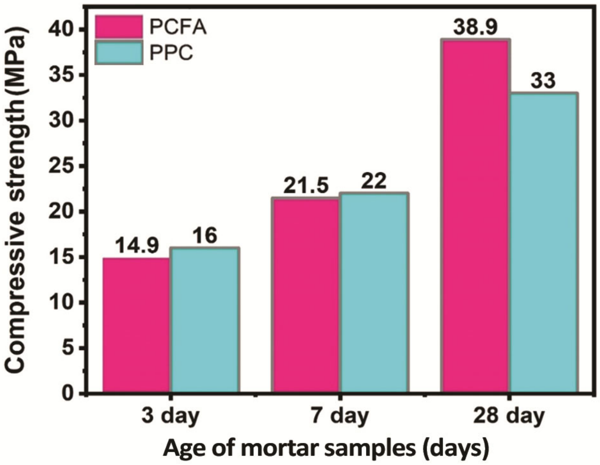

Fig. 12 — Average compressive strength vs age of mortar samples

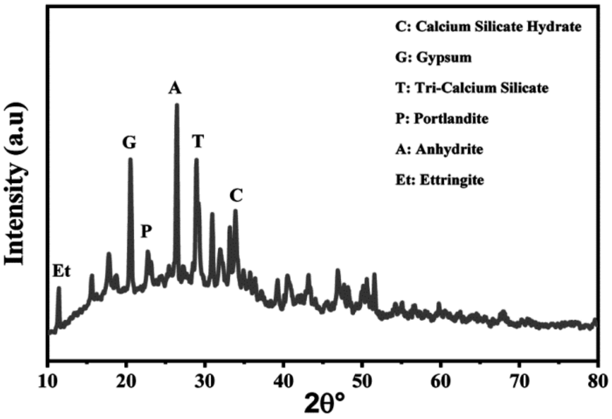

Fig. 13 — X- ray diffraction pattern for mortar sample

were calculated using Eq. 6. The strength of the mortar containing PCFA shows increasing trend, indicating that the usage of PCFA contributed to desirable strength development.

$$F = P/A \quad \dots (6)$$

where, F is compressive strength (MPa), P is maximum load (until failure), A is cross section of the area of the material resisting the load (mm^2)

The crushed mortar sample was analysed using XRD to identify the main hydration products. As shown in Fig. 13, it can be seen that the main hydration product found in the PCFA based mortar samples are Calcium Silicate Hydrate (C-S-H), Gypsum, Tri-Calcium Silicate, Portlandite, Anhydrite and Ettringite. The main peaks of C-S-H were seen at (2θ: 32.0°, 39.2° and 27.3°) and peaks of Tri-Calcium Silicate were seen at (2θ: 32.3°, 33.9°, 28.9°, 50.6° and 41.3°) whereas main peaks of Gypsum were seen at (2θ: 30.9°, 20.5° and 33.2°) and peaks of Anhydrite were seen at (2θ: 25.44°, 31.28°, 38.56°)

The improved reactivity of PCFA corresponds to improved strength in mortar containing PCFA.[33] PCFA-lime mortars were evaluated for compressive strength in accordance with IS 1727- 1967. The mix design is calculated using a 1:2M:9 (Specific Gravity of PCFA is 2.62 g/cc) proportion in which 395g of hydrated lime, 786 g of PCFA and 3537 g of sand mixed with sufficient water to create a flow of 70–75% in 6 seconds using 10 drops of the flow table. Mixing of sample shall be done at 27 ± 2°C. Three cube specimens of (50 × 50 × 50) mm^3 were casted for compressive strength testing. After casting, the samples were placed under wet gunny bag for 48 h along with the moulds. Then remove the moulds and cured in humidity chamber at 50 + 2°C for 8 days. Complete test procedure was followed as per IS 1727-1967. The average lime reactive compressive strength was found to be 8.6 MPa.

Several studies have reported that high calcium and sulphur content ash possess excellent pozzolanic properties and can be used as an alternative source for calcium aluminate cement.[34,35] Hence, similar possibilities arise in case of PCFA as it consists of high lime and SO_3 content. The existing ASTM C618(36) guidelines for categorising fly ash are applicable for conventional coal ash, where the SO_3 level is limited to 3–5 wt%. PCFA generated from the combustion of petroleum coke as fuel in CFBC boiler would not fall within the existing fly ash classification standard in terms of high SO_3 content i.e., 28%–40%. However, compressive strength is consistent with ASTM C593-06(37) requirements. Thus it can be used as an alternative binder for Pozzolanic material.

Conclusions

The Petcoke Fly Ash and Bed Ash are alkaline in nature due to high calcium content along with their fine particle size and chemical composition rich in lime and sulphite which are favourable for increasing self-cementitious property. XRD and FTIR analyses confirm the presence of cementitious phases in both ashes, supporting their potential for self-hardening. SEM and HR-TEM reveal a porous structure in PCFA, suggesting the need for primary treatment to reduce water demand. Leachate concentrations from both ashes are within permissible limits, indicating their non-hazardous nature. PCFA's fineness aligns with pozzolanic characteristics, contributing for faster strength development in concrete. Despite higher water requirement and longer setting time, PCFA shows promising compressive strength development, meeting ASTM C593-06 and IS 1489-1991 requirement, making it a viable alternative binder for pozzolanic materials in sustainable construction practices. Future research could expand through optimizing treatment methods to reduce water demand and further use as alternative binders in concrete by exploring their incorporation into building materials like bricks, pavers and tiles.

Acknowledgments

The authors are thankful to Prof. Avanish Kumar Srivastava, Director, CSIR-AMPRI, Bhopal for providing the lab facilities and permission to publish this work.

References

1 Henke K R, Trace element chemistry of fly ashes from co-combusted petroleum coke and coal, *Int Ash Util Symp, Center for Applied Energy Research*, University of Kentucky, Lexington, KY (2005).

2 Naga K S, Venkateswara R T & Deva K M L S, Design modelling for commercial/ pilot-scale circulating fluidized bed combustion (CFBC) boiler, *Int Conf Adv Mech Eng Mater Sci* ICAMEMS 2023. Singapore: Springer Nature Singapore (2023), **1–21**, https://doi.org/10.1007/978-981-99-5613-5_1.

3 Zhang W, Wang S, Ran J, Lin H, Kang W & Zhu J, Research progress on the performance of circulating fluidized bed combustion ash and its utilization in China, *J Build Eng*, **52** (2022) 104350, https://doi.org/10.1016/j.jobe.2022.104350.

4 Chen J & Lu X, Progress of petroleum coke combusting in circulating fluidized bed boilers — a review and future perspectives, *Resour Conserv Recycl*, **49(3)** (2007) 203–216, https://doi.org/10.1016/j.resconrec.2006.03.012.

5 Wang L, Hongzhu Q & Li Q, Effect of solid waste-petroleum coke residue on the hydration reaction and property of concrete, *Materials*, **12(8)** (2019) 1216, https://doi.org/10.3390/ma12081216.

6 Gonzalez A, Navia R & Moreno N, Fly ashes from coal and petroleum coke combustion: Current and innovative potential applications, *Waste Manag Res*, **27(10)** (2009) 976–987, https://doi.org/10.1177/0734242X09103190.

7 Ohenoja K, Pesonen J, Yliniemi J & Illikainen M, Utilization of fly ashes from fluidized bed combustion: A review, *Sustainability*, **12(7)** (2020) 2988, https://doi.org/10.3390/su12072988.

8 Jia G, Wang Y & Yang F, A review on the application of circulating fluidized bed fly ash in building materials, *Adv Mater Sci Eng*, **2022(1)** (2022) 7099430, https://doi.org/10.1155/2022/7099430.

9 Patel A, Basu P & Acharya B, An investigation into partial capture of CO_2 released from a large coal/petcoke fired circulating fluidized bed boiler with limestone injection using its fly and bottom ash, *J Environ Chem Eng*, **5(1)** (2017) 667–678, https://doi.org/10.1016/j.jece.2016.12.047.

10 He P, Zhang X, Chen H & Zhang Y, Waste-to-resource strategies for the use of circulating fluidized bed fly ash in construction materials: A mini review, *Powder Technol*, **393** (2021) 773–785, https://doi.org/10.1016/j.powtec.2021.08.035.

11 Basu P, *Fluidized bed boilers: design and application*, Elsevier (2013).

12 Indian standard method of physical tests for hydraulic cement, Determination of fineness of specific surface by blaine air permeability method, IS 4031(Part 2), Bureau of Indian Standards, New Delhi, India, 1999 (Reaffirmed 2004).

13 Indian standard methods of test for soils, Determination of specific gravity, section 1 fine grained soils, IS: 2720 (Part III/Sec 1), Bureau of Indian Standards, New Delhi, India, 1980 (Reaffirmed 2002).

14 Indian standard methods of test for soils, Determination of water content (second revision), IS: 2720 (Part II)-1973, Bureau of Indian Standards, New Delhi, India, 1973 (Reaffirmed 2010).

15 Indian Standard Methods of test for pozzolanic materials, Bureau of Indian Standard, New Delhi, 1727–1967 (Reaffirmed 2004).

16 EPA method 3050B: Acid digestion of sediments, sludges and soil, Revision 2, Washington, DC, December 1996.

17 EPA method 1311 (SW-846): Toxicity characteristic leaching procedure, July 1992.

18 Indian standard method of physical tests for hydraulic cement, Determination of consistency of standard cement paste, IS 4031 (Part 4) Bureau of Indian Standards, New Delhi, India, 1988 (Reaffirmed 2005).

19 Indian standard method of physical tests for hydraulic cement, Determination of compressive strength of hydraulic cement other than mansory cement, IS 4031 (Part 6) *Bureau of Indian Standards*, New Delhi, India, 1988 (Reaffirmed 2000).

20 Sheng G, Li Q, Zhai J & Li F, Self-cementitious properties of fly ashes from CFBC boilers co-firing coal and high-sulphur petroleum coke, *Cem Concr Res*, **37(6)** (2007) 871–876, https://doi.org/10.1016/j.cemconres.2007.03.013.

21 LiX G, Chen Q B, Huang K Z, Ma B G & Wu B, Cementitious properties and hydration mechanism of circulating fluidized bed combustion (CFBC) desulfurization ashes, *Constr Build Mater*, **36(4)** (2012) 182–187, https://doi.org/10.1016/j.conbuildmat.2012.05.017.

22 Lee S H & Kim G S, Self-cementitious hydration of circulating fluidized bed combustion fly ash, *J Korean Ceram Soc*, **54(2)** (2017) 128–136, https://doi.org/10.4191/kcers.2017.54.2.07.

23 Zhang W, Wang S, Ran J, Lin H, Kang W & Zhu J, Research progress on the performance of circulating fluidized bed combustion ash and its utilization in China, *J Build Eng*, **52** (2022) 104350, https://doi.org/10.1016/j.jobe.2022.104350.

24 Xun X, Xiaoling F & Chenglin Y, Investigation on physical properties, strength and phase evolution of binary cementitious materials made of CFBC ash and lime, *Constr Build Mater*, **265** (2020) 120302, https://doi.org/10.1016/j.conbuildmat.2020.120302.

25 Chen X, Xu Z, Yao Z, Shuai Q, Jiang Z, Peng X & Li H, Preparation of non-sintered lightweight aggregates through co-mechanochemical treatment of oil-contaminated drill

cuttings, circulation fluidized bed combustion fly ash, and quicklime, *Environ Sci Pollut Res*, **27** (2020) 20904–20911.

26 Paaver P, Paiste P, Liira M & Kirsimae K, Mechanical activation of the Ca-rich circulating fluidized bed combustion fly ash: Development of an alternative binder system, *Minerals*, **11(1)** (2020) 3, https://doi.org/10.3390/min11010003.

27 Pei J S F, Soh M, Choo C S, Ong D E L, Ng S M & Sunarso J, Harnessing fluidised bed combustion fly ash as a potential green binder: Origin, characteristics, mechanisms, and products properties, *Next Materials*, **1(2)** (2023) 100015, https://doi.org/10.1016/j.nxmate.2023.100015.

28 Kleinhans U, Wieland C, Frandsen F J & Spliethoff H, Ash formation and deposition in coal and biomass fired combustion systems: Progress and challenges in the field of ash particle sticking and rebound behaviour, *Prog Energy Combust Sci*, **68** (2018) 65–168, https://doi.org/10.1016/j.pecs.2018.02.001.

29 Singh K, Singh A K, Kumar A & Agarwal A, Fly ash and TiO_2 modified fly ash as adsorbing materials for effective removal of methylene blue and malachite green from aqueous solutions, *J Indian Chem Soc*, **10** (2023) 100256, https://doi.org/10.1016/j.hazadv.2023.100256.

30 Kalak T & Tachibana Y, Removal of lithium and uranium from seawater using fly ash and slag generated in the CFBC technology, *RSC Adv*, **11(36)** (2021) 21964–21978.

31 Indian standard of specification of portland pozzolana cement, IS 1489 (Part I) Bureau of Indian Standards, New Delhi, India, 1991 (Reaffirmed 2002).

32 ASTM C191 – 21, Standard test methods fortime of setting of hydraulic cement by vicat needle; 2021.

33 Pei S L, Pan S Y, Gao X, Fang Y K & Chiang P C, Efficacy of carbonated petroleum coke fly ash as supplementary cementitious materials in cement mortars, *J Clean Prod*, **180** (2018) 689–697, https://doi.org/10.1016/j.jclepro.2018.01.055.

34 Jewell R B, Rathbone R F, Duvallet T Y, Robl T L & Mahboub K C, Fabrication and testing of low-energy calcium sulfoaluminate-belite cements that utilize circulating fluidized bed combustion by-products, *Coal Combust Gasification Prod*, **7(2)** (2015) 9–18, https://doi.org/10.4177/CCGP-D 15-00001.1.

35 Marroccoli M, Pace M L, Telesca A, Valenti G L & Montagnaro F, Utilization of coal combustion ashes for the synthesis of ordinary and special cements, *Combust Sci Technol*, **182(4–6)** (2010) 588–599, https://doi.org/10.1080/00102200903466210.

36 ASTM C618, Standard specification for coal fly ash and raw or calcined natural pozzolana for use in concrete, American Society for Testing and Materials, 2012.

37 ASTM C593, Standard specification for fly ash and other pozzolana for use with lime for soil stabilization, American Society for Testing and Materials, 2011.